A Novel Vector-Based Pulse-Width Modulation for Cascaded H-Bridge Multilevel Inverters

T. Qanbari , B. Tousi [*], M. Farhadi-Kangarlu

Department of Electrical Engineering, Urmia University, Urmia, Iran

Abstract- *The conventional space vector pulse-width modulation (SVPWM) for cascaded H-bridge inverters (CHBIs) has problems of computational complexity and memory requirements. Operation in overmodulation mode is the other reason for the complexity in SVPWM. This paper proposes a novel modulation method, named as level vector pulse-width modulation (LVPWM), for voltage control of CHBIs. The concept of the proposed method is similar to the SVPWM but with different vector diagram and dwell times calculations. Unlike the SVPWM, the α and β axes and also their variables are considered separately without gathering in complex variables. The vector diagram has two separated α and β axes each of which contains individual switching vectors and reference vectors. The selection of the vectors to synthesize the reference vectors depends only on the amplitudes of the reference vectors. The computational overhead and memory requirement are independent of the number of cascaded H-bridges. Lower computational overhead and easy and continuous extension to overmodulation region are the advantages of the proposed method compared with the SVPWM-based methods. Moreover, the switching algorithm achieves improved efficiency for the inverter. Simulation and experimental results verify the effectiveness of the proposed algorithm.*

Keyword: Multilevel Inverter, Cascaded H-bridge Inverter, Space Vector Pulse-Width Modulation, Overmodulation.

NOMENCLATURE

SVPWM	Space vector pulse-width modulation
LVPWM	Level vector pulse-width modulation
CHBI	Cascaded H-bridge inverters
HBI	H-bridge inverter
V_m	Amplitude of the reference signals
ω	Angular frequency of the reference signals
φ	Phase delay angle of the reference signals
$V_{r\alpha}$	Voltage reference on α axis
$V_{r\beta}$	Voltage reference on β axis
V_α	Output voltage on α axis
V_β	Output voltage on β axis
m	Modulation index
V_{a1}	Fundamenental component of output voltage
T_s	Sampling time
f_s	Sampling frequency
f_o	Output voltage frequency
P_{sw}	Switching losses

1. INTRODUCTION

Cascaded H-bridge multilevel inverter is one of the main and popular topologies between the DC to AC converters. SVPWM is the more efficient method for voltage control of this converter due to its key characteristics like better DC voltage utilization, switching losses reduction, low output current harmonic components and easiness in digital implementation [1]-[4]. In spite of the mentioned advantages, SVPWM has problems including the computational complexity to identify the location of the reference voltage vector and the memory requirements of switching states and corresponding duty ratios. For a CHBI with n symmetrical H-bridges per phase, there are $(2n+1)$ levels for the output voltage of each phase, resulting in $(2n+1)^3$ switching states, $(12n^2+6n+1)$ vectors, and 24 n^2 triangles in the space vector diagram. These problems become critical for inverters with high number of output voltage levels [4]-[5].

In order to solve the mentioned problems, attractive methods have been proposed in the literature. A simplified SVPWM has been presented in [5]. Treating each unit as a three-level inverter and adopting serial calculation mode, a CHBI is modulated unit by unit using three-level SVPWM. A series SVPWM method for CHBIs that is based on the construction of multilevel reference vectors from three-level voltage vectors has been presented in Ref. [6]. In the generalized SVPWM proposed in Ref. [7], a method is presented to identify the center of a sub-hexagon containing the reference space vector. Using the center

of the sub-hexagon, the reference space vector is mapped to the innermost sub-hexagon, and the switching sequence corresponding to a two-level inverter is determined. Similarly, decomposing of the seven-level space vector hexagon of a CHBI into a number of two-level space vector hexagons has been proposed in [8]. A generalized SVPWM framework has been proposed in [9] based on the convenient definition of three non-orthogonal static reference frames, alternative to the $\alpha\beta$ frame. In the proposed SVPWM in [10], a method called the *l-factor* approach is proposed, which simplifies the determination of the space vector location in the space vector hexagon and online computations of the control pulses for multilevel inverters. Three techniques have been presented to simplify the identification of the nearest three vectors to the reference vector in [11]. The first two techniques are based on resolving the multilevel inverter space vector diagram into appropriate two-level hexagons. The third technique is an algorithm-based technique that makes use of a 60° spaced *g-h* coordinate system to perform the SVPWM of multilevel inverters. Another simplified method based on the 60° spaced *g-h* coordinate system has been proposed in [12]. In [13], a discontinuous SVPWM algorithm in the *abc* reference frame has been proposed for CHBIs. The *L*-level SVPWM problem is solved based on the two-level SVPWM one. A fast method based on the imaginary coordinate has been proposed in [14]. The advantage of this method over other methods is that it does not need to transform from the imaginary coordinate system back to the a-b-c (or α-β) coordinate in order to select the redundant vectors using look-up tables. The nearest-level-equivalent SVPWM method proposed in [15] has an attractive algorithm to obtain the modulation vectors based on the basic vectors. A simplified space vector pulse density modulation scheme has been proposed in [16]. The control strategy uses three sigma-delta modulators, wherein the reference space vector is vector quantized to generate the output switching vectors. The switching vectors for the inverters are derived without coordinate transformation and sector identification in this scheme, making the algorithm computationally simpler.

Overmodulation operation is one of the most important issues for PWM converters. In the SVPWM-based methods, overmodulation occurs as the reference vector goes beyond the circle inscribed in the hexagon in the vector diagram. However, a distortion of the output voltage occurs and the accurate value of its fundamental component cannot be obtained. The complexity of the SVPWM methods increases further in the overmodulation region due to the nonlinearity of this region [18]-[20]. Most of the simplified SVPWM methods also do not consider the overmodulation operation. The method proposed in [19] is one of the scant SVPWM methods for CHBIs which includes operation in overmodulation range.

The reviewed methods consider hexagonal SVPWM diagrams in complex coordinates and propose attractive methods for simplification of the reference vector location identification and switching pulses generation. This paper proposes a novel modulation method for CHBIs similar to SVPWM concept but with different vector diagram and dwell times calculations to solve the mentioned problems associated with the SVPWM method. In the proposed method, the variables on α and β axes are not gathered in complex variables. The vector diagram has two separated α and β axes each of which contains individual switching vectors and reference vectors. The selection of the vectors to synthesize the reference vectors depends only on the amplitudes of the reference vectors. The proposed scheme has a simple algorithm and can be implemented even on an ordinary microcontroller. This method has been applied to a computer-aided simulated and laboratory-built CHBI. The effectiveness of the method has been verified by simulation and experimental results.

2. PRINCIPLE of The PROPOSD METHOD

Principle of the proposed method for CHBIs is presented with a three-phase three-level H-bridge inverter (HBI). The circuit diagram of an HBI is shown in Fig. 1. The sinusoidal references for the phase voltages of the inverter load are as follows:

$$V_{rao}(t) = V_m \sin(\omega t + \varphi) \tag{1}$$

$$V_{rbo}(t) = V_m \sin\left(\omega t - \frac{2\pi}{3} + \varphi\right), \tag{2}$$

$$V_{rco}(t) = V_m \sin\left(\omega t + \frac{2\pi}{3} + \varphi\right). \tag{3}$$

where V_m is the amplitude, ω is the angular frequency and φ is the phase delay angle. It is possible to transform these voltage references to equivalent two-phase variables using Clarke transformation [1]:

$$\begin{bmatrix} V_{r\alpha}(t) \\ V_{r\beta}(t) \end{bmatrix} = \frac{2}{3} \begin{bmatrix} 1 & -\frac{1}{2} & -\frac{1}{2} \\ 0 & \frac{\sqrt{3}}{2} & -\frac{\sqrt{3}}{2} \end{bmatrix} \begin{bmatrix} V_{rao}(t) \\ V_{rbo}(t) \\ V_{rco}(t) \end{bmatrix}. \tag{4}$$

According to this transformation, $V_{r\alpha}$ and $V_{r\beta}$ are

$$V_{r\alpha}(t) = \frac{2}{3}\left(v_{rao} - \frac{1}{2}(v_{rbo} + v_{rco})\right) = V_m \sin(\omega t + \varphi), \tag{5}$$

$$V_{r\beta}(t) = \frac{\sqrt{3}}{3}(v_{rbo} - v_{rco}) = -V_m \cos(\omega t + \varphi). \tag{6}$$
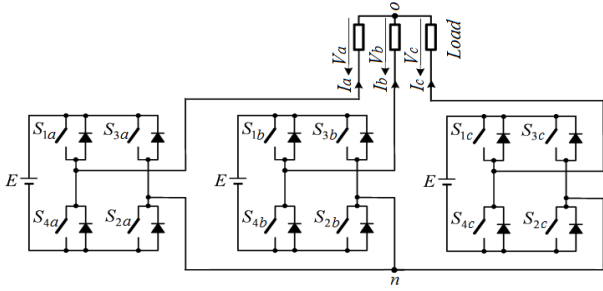
Fig. 1. Circuit diagram of the three-phase three-level HBI

Table 1. The switching states, the corresponding load voltages and the Clarcke transformation of these voltages

Switching States	v_a	v_b	v_c	V_α	V_β
PPP	0	0	0	$0(V_{\alpha1})$	$0(V_{\beta1})$
PPO	E/3	E/3	-2E/3	$E/3(V_{\alpha4})$	$\sqrt{3}E/3(V_{\beta4})$
PPN	2E/3	2E/3	-4E/3	$2E/3(V_{\alpha9})$	$2\sqrt{3}E/3(V_{\beta9})$
POP	E/3	-2E/3	E/3	$E/3(V_{\alpha5})$	$-\sqrt{3}E/3(V_{\beta5})$
POO	2E/3	-E/3	-E/3	$2E/3(V_{\alpha8})$	$0(V_{\beta8})$
PON	E	0	-E	$E(V_{\alpha14})$	$\sqrt{3}E/3(V_{\beta14})$
PNP	2E/3	-4E/3	2E/3	$2E/3(V_{\alpha10})$	$-2\sqrt{3}E/3(V_{\beta10})$
PNO	E	-E	0	$E(V_{\alpha15})$	$-\sqrt{3}E/3(V_{\beta15})$
PNN	4E/3	-2E/3	-2E/3	$4E/3(V_{\alpha18})$	$0(V_{\beta18})$
OPP	-2E/3	E/3	E/3	$-2E/3(V_{\alpha11})$	$0(V_{\beta11})$
OPO	-E/3	2E/3	-E/3	$-E/3(V_{\alpha6})$	$\sqrt{3}E/3(V_{\beta6})$
OPN	0	E	-E	$0(V_{\alpha2})$	$2\sqrt{3}E/3(V_{\beta2})$
OOP	-E/3	-E/3	2E/3	$-E/3(V_{\alpha7})$	$-\sqrt{3}E/3(V_{\beta7})$
OOO	0	0	0	$0(V_{\alpha1})$	$0(V_{\beta1})$
OON	E/3	E/3	-2E/3	$E/3(V_{\alpha4})$	$\sqrt{3}E/3(V_{\beta4})$
ONP	0	-E	E	$0(V_{\alpha3})$	$-2\sqrt{3}E/3(V_{\beta3})$
ONO	E/3	-2E/3	E/3	$E/3(V_{\alpha5})$	$-\sqrt{3}E/3(V_{\beta5})$
ONN	2E/3	-E/3	-E/3	$2E/3(V_{\alpha8})$	$0(V_{\beta8})$
NPP	-4E/3	2E/3	2E/3	$-4E/3(V_{\alpha19})$	$0(V_{\beta19})$
NPO	-E	E	0	$-E(V_{\alpha16})$	$\sqrt{3}E/3(V_{\beta16})$
NPN	-2E/3	4E/3	-2E/3	$-2E/3(V_{\alpha13})$	$2\sqrt{3}E/3(V_{\beta13})$
NOP	-E	0	E	$-E(V_{\alpha17})$	$-\sqrt{3}E/3(V_{\beta17})$
NOO	-2E/3	E/3	E/3	$-2E/3(V_{\alpha11})$	$0(V_{\beta11})$
NON	-E/3	2E/3	-E/3	$-E/3(V_{\alpha6})$	$\sqrt{3}E/3(V_{\beta6})$
NNP	-2E/3	-2E/3	4E/3	$-2E/3(V_{\alpha12})$	$-2\sqrt{3}E/3(V_{\beta12})$
NNO	-E/3	-E/3	2E/3	$-E/3(V_{\alpha7})$	$-\sqrt{3}E/3(V_{\beta7})$
NNN	0	0	0	$0(V_{\alpha1})$	$0(V_{\beta1})$

Using this transformation, the inverter has two voltage references. There are 27 possible combinations of switching states in the HBI. The switching states, the corresponding load voltages and the Clarke transformations of these voltages are listed in Table 1. The switching state 'P' denotes that the S_1 and S_2 switches in each H-bridge are on and then the output voltage of the H-bridge is equal to E. The switching state 'N' denotes that the S_3 and S_4 switches in each H-bridge are on and then the output voltage of the H-bridge is equal to $-E$. The switching state 'O' denotes that the S_1 and S_2 switches or S_3 and S_4 switches in each

H-bridge are on and then the output voltage of the H-bridge is equal to zero. Fig. 2 shows the transformed values of the voltages references ($V_{r\alpha}$ and $V_{r\beta}$) and also the transformed values of the load voltages of the inverter (V_α and V_β) for each switching state. As listed in Table 1 and shown in Fig. 2, V_α and V_β are defined by vectors ($V_{\alpha1}$ to $V_{\alpha19}$ and $V_{\beta1}$ to $V_{\beta19}$) for each switching state. Each vector represents a level in the V_α and V_β waveforms. Hence, these vectors are named level vectors. Some of the switching states have equal values of V_α and V_β. In other words, some of V_α and V_β vectors have redundant switching states. Each of the voltage references ($V_{r\alpha}$ and $V_{r\beta}$) also can be modeled by a vector. Fig. 3 shows the level vectors and the reference vectors on the α and β axes. This figure is the vector diagram of the proposed modulation method. This vector diagram has two separated α and β axes each of which contains individual switching vectors and reference vectors. The level vectors are fixed and the amplitudes of the reference vectors vary sinusoidally. The selection of the vectors to synthesize the reference vectors depends on only the amplitudes of the reference vectors. In order to produce the desired output voltage, the inverter must synthesize the reference vectors by the level vectors at each sampling period by proper selection of the switching states.

Similar to the SVPWM, three nearby level vectors synthesize the reference vectors during a sampling period (T_s) in the proposed method. As an example, Fig. 4 shows the synthesis of V_α by $V_{\alpha5}$, $V_{\alpha3}$ and $V_{\alpha7}$ and the synthesis of V_β by $V_{\beta5}$, $V_{\beta3}$ and $V_{\beta7}$. Each switching state has a dwell time in the sampling period. The dwell times values must be calculated such that the integral of V_α be equal to the integral of $V_{r\alpha}$ and also the integral of V_β be equal to the integral of $V_{r\beta}$ in the sampling period as follows:

$$A_{\alpha1} + A_{\alpha2} + A_{\alpha3} = A_{\alpha r}, \tag{7}$$
$$A_{\beta1} + A_{\beta2} + A_{\beta3} = A_{\beta r}, \tag{8}$$

where $A_{\alpha1}$, $A_{\alpha2}$ and $A_{\alpha3}$ are the areas of V_α for each of the three selected switching states, $A_{\beta1}$, $A_{\beta2}$ and $A_{\beta3}$ are the areas of V_β for each of the three selected switching states and $A_{\alpha r}$ and $A_{\beta r}$ are the areas $V_{r\alpha}$ and $V_{r\beta}$ in the sampling period. $A_{\alpha r}$ and $A_{\beta r}$ can be calculated as follows:

$$A_{\alpha r} = I_{\alpha r} = \int_{t_0}^{t_0+T_S} V_{\alpha r} \, dt = \frac{V_m}{\omega}[cos(\omega t_0 + \varphi) - cos(\omega t_0 + \omega T_S + \varphi)] \tag{9}$$

$$A_{\beta r} = I_{\beta r} = \int_{t_0}^{t_0+T_S} V_{\beta r} \, dt = \frac{V_m}{\omega}[sin(\omega t_0 + \varphi) - sin(\omega t_0 + \omega T_S + \varphi)] \tag{10}$$

where t_0 is the starting point of each sampling period.
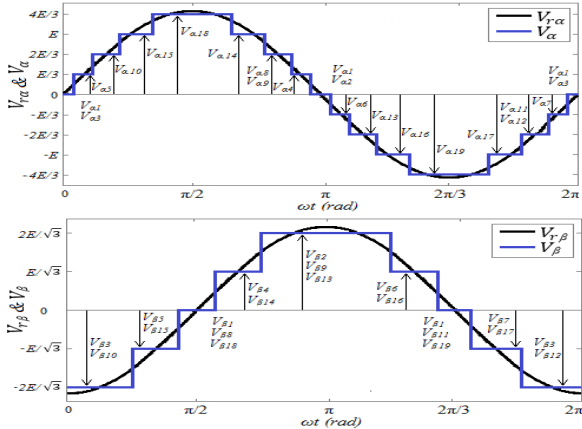
Fig. 2. The transformed values the voltages references and the transformed values the load voltages of the inverter for each switching state
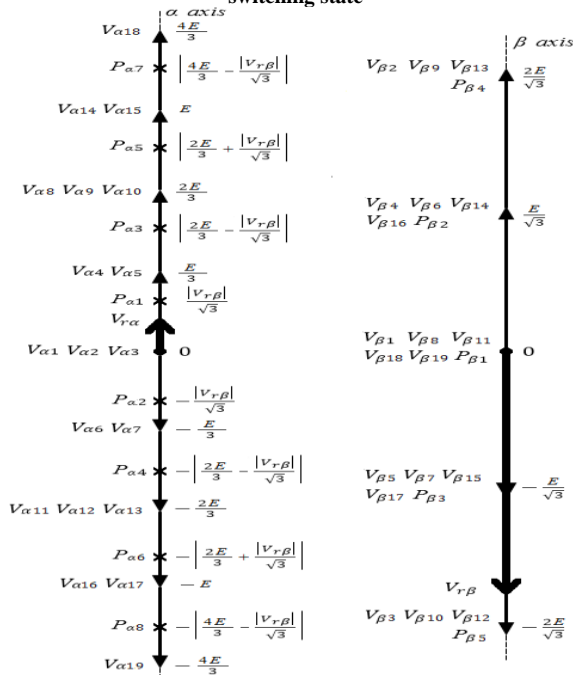
Fig. 3. Vector diagram of the proposed modulation method
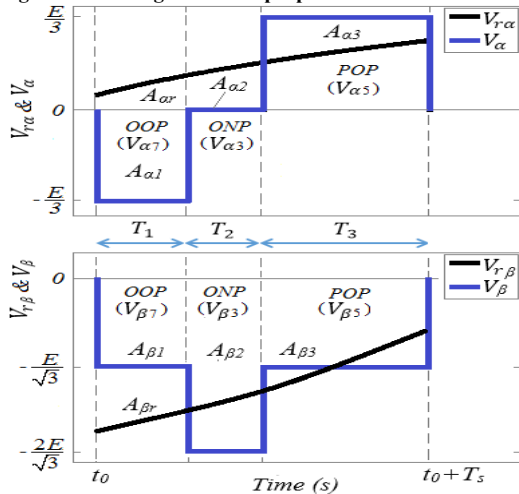
Fig. 4. An example of the synthesis of $V_{r\alpha}$ and $V_{r\beta}$ by V_α and V_β in one sampling period

Then, the following system of equations gives the dwell times values of the selected vectors:

$$\begin{cases} V_{s\alpha 1}T_1 + V_{s\alpha 2}T_2 + V_{s\alpha 3}T_3 = I_{\alpha r} \\ V_{s\beta 1}T_1 + V_{s\beta 2}T_2 + V_{s\beta 3}T_3 = I_{\beta r} \\ T_1 \;+\; T_2 \;+\; T_3 = T_s \end{cases} \qquad (11)$$

where Vsα1, Vsα2 and Vsα3 are the three selected vectors from α axis, Vsβ1, Vsβ2 and Vsβ3 are the three selected vectors from β axis and T1, T2 and T3 are the dwell times of the corresponding switching states of these vectors in the sampling period respectively. Vsα1, Vsα2 and Vsα3 have common switching states with Vsβ1, Vsβ2 and Vsβ3 respectively. Obviously, the dwell times values must be positive. So, the above system of equations specifies which of the level vectors must be selected to synthesize the reference vectors. The selection of the proper level vectors at each sampling period depends on the values and locations of the reference vectors. Solving Eq. (11) denotes that each group of the level vectors has positive dwell time values for definite and limited values of the reference vectors. The points Pα1, to Pα8 divide the α axis into nine regions and the points Pβ1 to Pβ5 divide the β axis into six regions. These points have the following values:

$$P_{\alpha 1} = -P_{\alpha 2} = \frac{|v_{r\beta}|}{\sqrt{3}}, \qquad (12)$$

$$P_{\alpha 3} = -P_{\alpha 4} = \left| \frac{2E}{3} - \frac{|v_{r\beta}|}{\sqrt{3}} \right|, \qquad (13)$$

$$P_{\alpha 5} = -P_{\alpha 6} = \left| \frac{2E}{3} + \frac{|v_{r\beta}|}{\sqrt{3}} \right|, \qquad (14)$$

$$P_{\alpha 7} = -P_{\alpha 8} = \left| \frac{4E}{3} - \frac{|v_{r\beta}|}{\sqrt{3}} \right|, \qquad (15)$$

$$P_{\beta 1} = 0, \qquad (16)$$

$$P_{\beta 2} = -P_{\beta 3} = \frac{E}{\sqrt{3}}, \qquad (17)$$

$$P_{\beta 4} = -P_{\beta 5} = \frac{2E}{\sqrt{3}}. \qquad (18)$$

In each region between these points, there is a group of the level vectors that satisfy Eq. (11) to synthesize the reference vectors. Depending on the values and locations of the reference vectors, the admissible level vectors to be selected to synthesize the reference vectors are listed in Table 2. Between the admissible level vectors, the vectors with common switching states are the selected vectors to synthesize the reference vectors in each sampling period. For example, at the locations of the reference vectors in Fig. 3, the vectors $V_{\alpha 1}$, $V_{\alpha 2}$, $V_{\alpha 3}$, $V_{\alpha 4}$, $V_{\alpha 5}$, $V_{\alpha 6}$ and $V_{\alpha 7}$ are the admissible vectors to synthesize $V_{r\alpha}$ and the vectors $V_{\beta 5}$, $V_{\beta 7}$, $V_{\beta 15}$, $V_{\beta 17}$, $V_{\beta 3}$, $V_{\beta 10}$ and $V_{\beta 12}$ are the admissible vectors to synthesize $V_{r\beta}$. Between these vectors, $V_{\alpha 3}$ with $V_{\beta 3}$, $V_{\alpha 5}$ with $V_{\beta 5}$ and $V_{\alpha 7}$ with $V_{\beta 7}$ have the common switching states. Then, these vectors are the proper vectors to synthesize the reference vectors at these points. Fig. 5 shows a sample of the V_α and V_β waveforms synthesized by the

proposed method in one cycle.

After selecting the level vectors and calculating their dwell times, switching sequence arranging is the next step. The aim of a proper switching sequence design is to minimize the switching frequencies of the devices. Fig. 6 shows a sample of seven-segment switching sequence in the proposed modulation. At each transition from one switching state to the next, only one switch turns on and one switch turns off in each H-bridge. Utilizing the redundant switching states, the number of the switchings reduces. So the switching frequency of the devices is thus equal to the sampling frequency. According to Eq. (12) to Eq. (18), the maximum value for both V_{ra} and $V_{r\beta}$ to satisfy the system of equations (11) is $2\sqrt{3}E/3$. For higher values, the system of equations gives negative values for dwell times. The amplitudes of the voltage references in modulation region can vary from $2\sqrt{3}E/3$ down to $-2\sqrt{3}E/3$ as follows:

$$V_m = m\frac{2\sqrt{3}}{3}E, \qquad 0 \le m \le 1 \qquad (19)$$

where m is the modulation index. Similar to the conventional SVPWM method, there is a linear relationship between the output voltage and the input DC voltage in the range of $0 \le m \le 1$. In order to produce output voltage with higher values, the inverter operation extends to overmodulation. For values of m higher than 1, the reference vectors may lie in regions out of the modulation regions of the proposed method diagram (Fig. 3 and Table 2) in some time intervals. These regions are overmodulation regions. When at least one of the reference vectors lies in overmodulation regions of the diagram, they cannot be synthesized by three level vectors. In other words, there is not any group of level vectors to satisfy (11). So, only one of the level vectors which is the closest vector to the reference vectors in each axis is the admissible vector to be selected. The admissible level vectors to synthesize the reference vectors in these regions are also listed in Table 2. The principle of the proposed method for overmodulation operation is similar to the presented linear modulation operation. Depending on the reference vectors locations, the number of the admissible level vectors with common switching states may be three or one. Then, the proposed method has two strategies for overmodulation mode:

1) If both of the reference vectors lie in the modulation region, operates similar to linear modulation operation. Selection of three level vectors and computation of the dwell times according to Eq. (11).

2) If at least one of the reference vectors lies in the overmodulation region, selects only one level vector in the sampling time period.

Fig. 7 shows a sample of the V_α and V_β waveforms synthesized by the proposed method in overmodulation mode. For V_m values high than *4E/3*, the inverter operates in overmodulation mode at all times, generating staircase output voltage.

The fundamental component of the phase a voltage of the load in overmodulation mode can be expressed using Fourier decomposition as follows:

$$V_{a1} = \frac{1}{\pi}\int_0^{2\pi} V_\alpha(\omega t)\sin(\omega t)\,d\omega t$$
$$= \frac{4}{\pi}\int_{\theta_1}^{\theta_2} V_m\sin^2(\omega t)d\omega t + \frac{4}{\pi}\int_{\theta_2}^{\theta_3} E\sin(\omega t)\,d\omega t +$$
$$\frac{4}{\pi}\int_{\theta_3}^{\frac{\pi}{2}} V_m\sin^2(\omega t)d\omega t \qquad (20)$$

Table 2. The regions on the axes and the admissible level vectors to synthesize the reference vectors

Region on α Axis	Admissible Vectors to Synthesize $V_{\alpha r}$	Region on β Axis	Admissible Vectors to Synthesize $V_{\beta r}$
$P_{\alpha2} \le V_{ra} \le P_{\alpha1}$ and $P_{\alpha4} \le V_{ra} \le P_{\alpha3}$	$V_{\alpha4}, V_{\alpha5}, V_{\alpha1}, V_{\alpha2}, V_{\alpha3}, V_{\alpha6}, V_{\alpha7}$	$P_{\beta2} \le V_{r\beta} \le P_{\beta4}$	$V_{\beta2}, V_{\beta9}, V_{\beta13}, V_{\beta4}, V_{\beta6}, V_{\beta14}, V_{\beta16}$
$P_{\alpha1} \le V_{ra} \le P_{\alpha3}$ or $P_{\alpha3} \le V_{ra} \le P_{\alpha1}$	$V_{\alpha8}, V_{\alpha9}, V_{\alpha10}, V_{\alpha4}, V_{\alpha5}, V_{\alpha1}, V_{\alpha2}, V_{\alpha3}$	$P_{\beta1} \le V_{r\beta} \le P_{\beta2}$	$V_{\beta4}, V_{\beta6}, V_{\beta14}, V_{\beta16}, V_{\beta1}, V_{\beta8}, V_{\beta11}, V_{\beta18}, V_{\beta19}$
$P_{\alpha1} \le V_{ra} \le P_{\alpha7}$ and $P_{\alpha3} \le V_{ra} \le P_{\alpha5}$	$V_{\alpha4}, V_{\alpha5}, V_{\alpha8}, V_{\alpha9}, V_{\alpha10}, V_{\alpha14}, V_{\alpha15}$	$P_{\beta3} \le V_{r\beta} \le P_{\beta1}$	$V_{\beta1}, V_{\beta8}, V_{\beta11}, V_{\beta18}, V_{\beta19}, V_{\beta5}, V_{\beta7}, V_{\beta15}, V_{\beta17}$
$P_{\alpha5} \le V_{ra} \le P_{\alpha7}$	$V_{\alpha8}, V_{\alpha9}, V_{\alpha10}, V_{\alpha14}, V_{\alpha15}, V_{\alpha18}$	$P_{\beta5} \le V_{r\beta} \le P_{\beta3}$	$V_{\beta5}, V_{\beta7}, V_{\beta15}, V_{\beta17}, V_{\beta3}, V_{\beta10}, V_{\beta12}$
$V_{ra} > P_{\alpha7}$	$V_{\alpha14}, V_{\alpha15}, V_{\alpha18}$	$V_{r\beta} > P_{\beta4}$	$V_{\beta2}, V_{\beta9}, V_{\beta13}$
$P_{\alpha4} \le V_{ra} \le P_{\alpha2}$ or $P_{\alpha2} \le V_{ra} \le P_{\alpha4}$	$V_{\alpha1}, V_{\alpha2}, V_{\alpha3}, V_{\alpha6}, V_{\alpha7}, V_{\alpha11}, V_{\alpha12}, V_{\alpha13}$	$V_{r\beta} < P_{\beta5}$	$V_{\beta3}, V_{\beta10}, V_{\beta12}$
$P_{\alpha8} \le V_{ra} \le P_{\alpha1}$ and $P_{\alpha6} \le V_{ra} \le P_{\alpha4}$	$V_{\alpha6}, V_{\alpha7}, V_{\alpha11}, V_{\alpha12}, V_{\alpha13}, V_{\alpha16}, V_{\alpha17}$		
$P_{\alpha8} \le V_{ra} \le P_{\alpha6}$	$V_{\alpha11}, V_{\alpha12}, V_{\alpha13}, V_{\alpha16}, V_{\alpha17}, V_{\alpha19}$		
$V_{ra} < P_{\alpha8}$	$V_{\alpha16}, V_{\alpha17}, V_{\alpha19}$		

The θ angles correspond to the confluences of the reference vectors and the points P on the α and β axis. At θ_1, $V_{r\beta}$ enters in the overmodulation region with the value higher than $P_{\beta5}$. Between θ_2 and θ_3, V_{ra} lies in the overmodulation region with the value higher than $P_{\beta7}$. This equation gives the relation of V_m and V_{a1} in overmodulation region. Unlike hexagonal space vector diagram, the level vector diagram has a simple linear topology such that identification of the reference vectors locations to select the proper switching states is simple with any number of vectors.
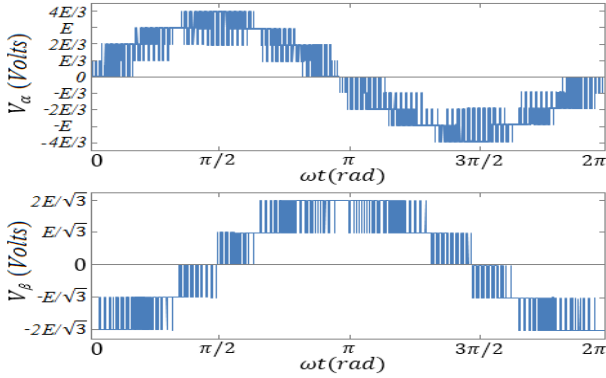
Fig. 5. V_α and V_β waveforms synthesized by the proposed method in one cycle
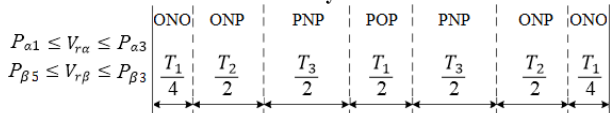
Fig. 6. A sample of switching sequence in the proposed modulation
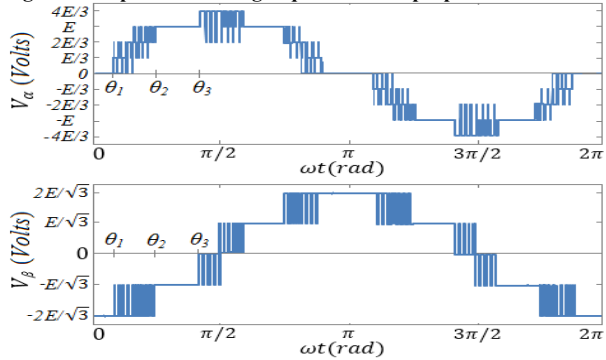
Fig. 7. V_α and V_β waveforms synthesized by the proposed method in overmodulation mode

3. LEVEL VECTOR PULSE-WIDTH MODULATION FOR CASCADED H-BRIDGE MULTILEVEL INVERTERS

3.1. Series LVPWM method

The circuit diagram of a symmetrical CHBI is shown in Fig. 8. This inverter contains n similar H-bridges in each phase. The CHBI has a modular topology and the level vector diagrams of the HBIs are the same. Then, only the level vector diagram of one HBI can be used for the overall system. The three-phase output voltages of the inverter are the sum of the three-phase output voltages of HBIs. The proposed method for the HBI can be generalized and implemented for CHBIs similar to the nearest level modulation of hybrid multilevel inverters. In the proposed method, the modulations of the HBIs are done separately and respectively similar to hybrid multilevel inverters [20]-[22]. Firstly, the HBI1 synthesizes the Vrα and Vrβ reference vectors. Then, the differences of the reference vectors and the output voltages of the HBI1 are the reference vectors of the HBI2 and so on. Generally, the reference vectors of the HBIs have the following values:

$$V_{r\alpha 1} = V_{r\alpha} \tag{21}$$

$$V_{r\beta 1} = V_{r\beta} \tag{22}$$

$$V_{r\alpha k} = \begin{cases} 0, & P_{\alpha 8} \leq V_{r\alpha(k-1)} \leq P_{\alpha 7} \ and \ P_{\beta 5} \leq V_{r\beta(k-1)} \leq P_{\beta 4} \\ V_{r\alpha(k-1)} - V_{\alpha k}, & otherwise \end{cases} \tag{23}$$

$$V_{r\beta k} = \begin{cases} 0, & P_{\alpha 8} \leq V_{r\alpha(k-1)} \leq P_{\alpha 7} \ and \ P_{\beta 5} \leq V_{r\beta(k-1)} \leq P_{\beta 4} \\ V_{r\beta(k-1)} - V_{\beta k}, & otherwise \end{cases} \tag{24}$$

where $V_{r\alpha k}$ and $V_{r\beta k}$ are the reference vectors of the k'th HBI. According to the above equations, when the reference vectors of an HBI are standing in the modulation region, that HBI synthesizes the reference vectors and the differences of that HBI output voltages and the reference vectors are zero in each sampling time. When one of the reference vectors lies in the over modulation regions, that HBI operates in over modulation mode and the differences of the HBI output voltages and the reference vectors are the reference vectors for the next HBI. Fig. 9 illustrates the proposed method graphically for a CHBI with three HBIs. In the proposed method, the HBIs operate in over modulation mode except the last HBI when the CHBI operates in linear modulation mode. In the example shown in Fig. 9, the HBI1 and HBI2 modules are in over modulation mode and HBI3 operates in linear modulation region. In over modulation mode, the last HBI also operates in over modulation mode. With this pattern, the supplied powers, the switching frequency and the conduction times are not the same for the H-bridge cells. To evenly distribute the supplied powers and also the switching losses, the switching pattern can be changed alternatively among the HBIs.
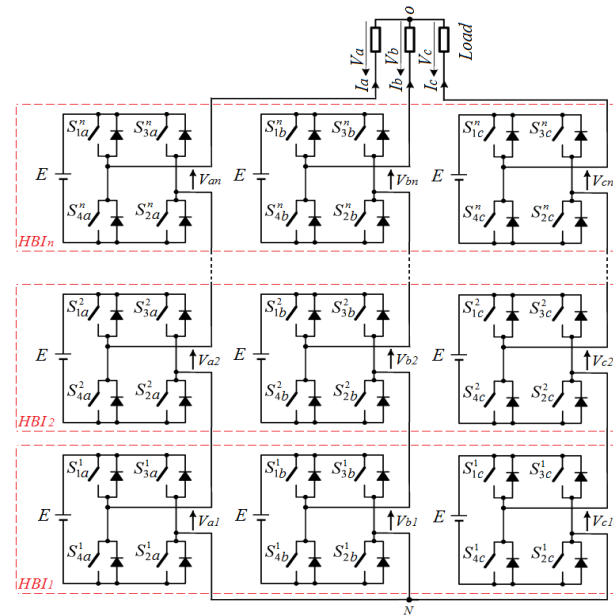
Fig. 8. Circuit diagram of the symmetrical CHBI with n HBIs
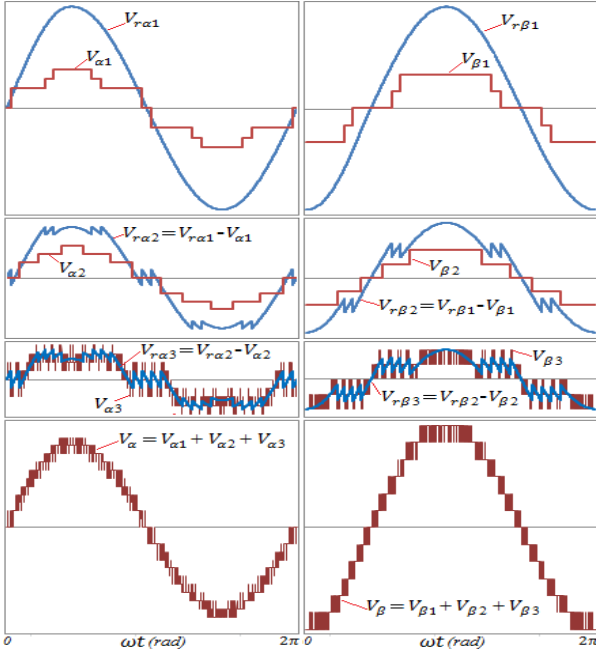
Fig. 9. Illustration of the proposed method with a CHBI with three HBIs

According to Eq. (19), the amplitude of the load phase voltage of the CHBI with n HBIs, in linear modulation region is

$$V_m = nm\frac{2\sqrt{3}}{3}E, \qquad 0 \leq m \leq 1. \qquad (25)$$

In overmodulation mode, the amplitude of the load phase voltage of the CHBI can be achieved from Eq. (20) as follows:

$$V_{a1} = V_{\alpha 11} + \cdots + V_{\alpha 1k} + \cdots + V_{\alpha 1n} \qquad (26)$$

where $V_{\alpha lk}$ is the fundamental component of V_α generated by the k'th HBI calculated from Eq. (20).

3.2. Features and comparisons
The proposed method has the following advantages:

1) The proposed method is a vector-based modulation technique and has all the advantages of SVPWM including easier digital implementation, higher DC voltage utilization, online implementation and flexibility in switching. The control signals of the proposed method can be changed online at any time. This feature is very important in control systems. Similar to SVPWM, the proposed method uses redundant switching states to reduce switching losses.

2) The LVPWM for CHBIs has a very low computational overhead and memory requirement. Fig. 10 shows the space vector diagram of a seven-level CHBI with three HBIs [11]. This diagram contains 127 vectors, 343 switching states and 216 triangles. Implementation of SVPWM with such a diagram is a cumbersome process even with the simplified methods.

As discussed, implementation of the LVPWM for CHBIs with any number of HBIs requires only the simple vector diagram shown in Fig. 3.

3) In the conventional and simplified [7]-[15] SVPWM methods, all of the switching states and space vectors of CHBI must be considered in design of the modulation strategy. In the proposed LVPWM, it is enough to consider switching states and level vectors of a three-level HBI for a CHBI with any number of cascaded HBIs.

4) The proposed method conveniently selects the switching vectors in the overmodulation condition and hence results in a smooth transition from linear to overmodulation region without requiring lookup tables.

5) Only one HBI operates with high switching frequency (the sampling frequency) and the switching frequencies of the other HBIs are equal to the fundamental frequency resulting higher efficiency for the CHBI similar to hybrid multilevel inverters [19]-[21].

3.3. Implementation
The proposed LVPWM method is a real-time modulation technique with easy digital implementation. Implementation of this method has the following steps:

1) Receiving the reference signals (Vrα and Vrβ).

2) Selecting proper level vectors to synthesize the reference vectors according to Table 2.

3) Computing dwell times values from Eq. (11) if three level vectors are selected at the sampling time.

4) Calculating the reference signals of the next HBI (equations 21 to 24).

5) Producing gate signals with switching sequence design considerations at each sampling time.

The flowchart of the proposed algorithm is shown in Fig. 11.

4. SIMULATION AND EXPERIMENTAL RESULTS
A CHBI with three symmetrical HBI modules with the characteristics given in table 3 and controlled by the proposed LVPWM method is simulated and implemented. The simulations are performed using Matlab/Simulink. Fig. 12 shows a picture of the prototype. The semiconductor switches are the half-bridge IGBT modules (LS LUH75G1202). The LVPWM method has been implemented by ezDSPro F2812 board (TMS320F2812). The sampling frequency

is 3 kHz. The required drive board is designed using HCPL-316J which is a fast and intelligent IGBT driver. The DC sources have been provided by multi-winding transformers and diode-bridge rectifiers. The inverter supplies a laboratory-built three-phase resistive-inductive load.

Table 3. Characteristics of the prototype

Item	Value
Output voltage (L-L RMS, f_o)	0-430 V , 1-150 Hz
Sampling frequency	3 kHz
Input DC voltages	90 V
Load	R= 10 Ω , L= 21 mH
The switches characteristics	IGBT, 1200V, 75A
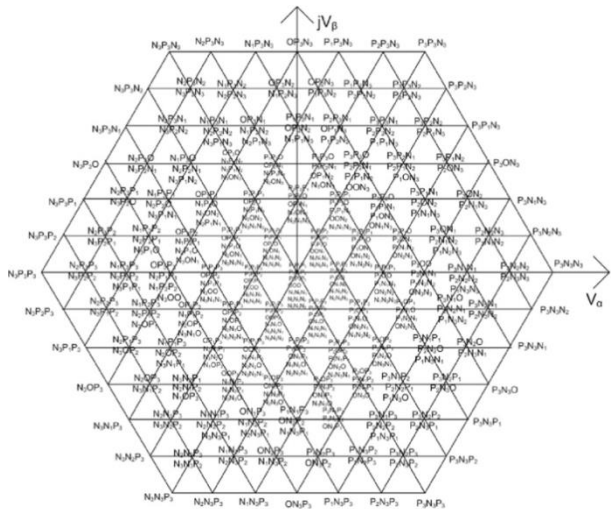
Fig. 10. Space vector diagram of a seven-level CHBI
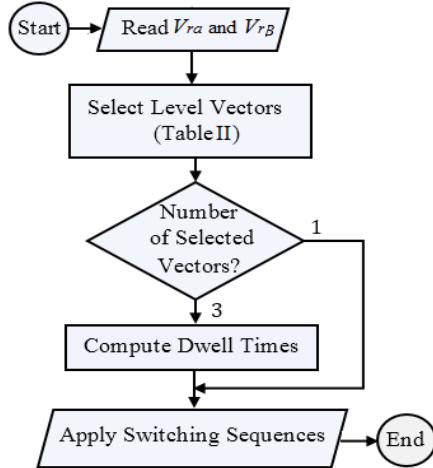
Fig. 11. Flowchart of the proposed algorithm
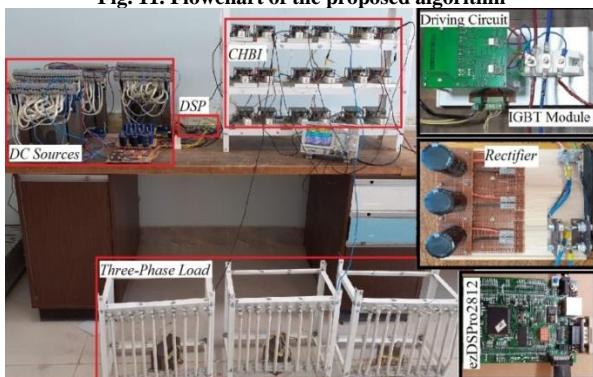
Fig. 12. Experimental setup

Fig. 13 shows the simulated switching pulses of the devices, output voltages of the H-bridge cells and phase voltage of the CHBI in linear modulation mode (m=0.96) in phase b. To evenly distribute the supplied powers and also the switching and conduction losses, the switching pattern for the devices in the H-bridge cells rotates in each phase. In other words, the switching pulses of the H-bridge cells change respectively in each three cycles. Fig. 14 shows the experimental output voltage of one of the H-bridge cells in phase a and the phase a voltage of the inverter for m=0.96. These figures show how the output voltages of the H-bridge cells synthesize the output voltage of the CHBI. Moreover, as shown in these figures, the H-bridge cells operate with the fundamental frequency (f_o) in two cycles and operate with the sampling frequency (f_s) in one cycle from each three cycles of operation. The switching losses of the switches are proportional to the switching frequency as follows [23]:

$$P_{sw} = (E_{on} + E_{off}) \times f_s \qquad (27)$$

where E_{on} and E_{off} are energy losses during on and off time periods of the switches respectively. So, the switching losses of the CHBI are almost 1/3 of the cases that the H-bridges operate with the sampling frequency all the time. The efficiency of the CHBI (the output power to the input power relation) is 98.3% at nominal conditions. This algorithm achieves an improved efficiency of the CHBI.
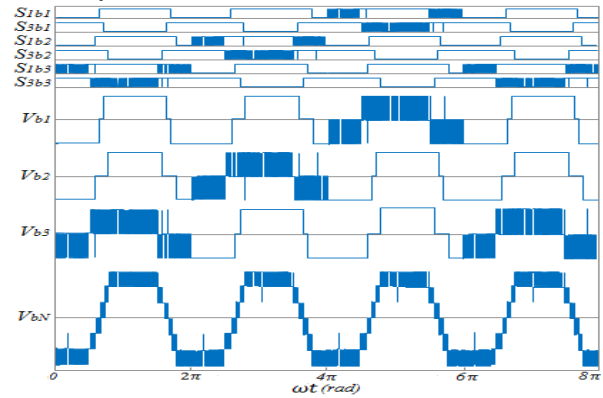
Fig. 13. Simulated switching pulses of the devices, output voltages of the H-bridge cells and phase voltage of the CHBI in linear modulation mode
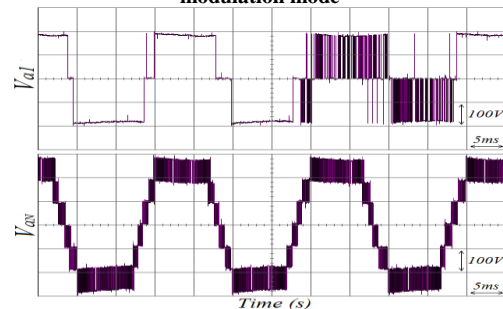
Fig. 14. Experimental output voltage of one of the H-bridge cells in the phase a and the phase a voltage of the inverter for m=0.96
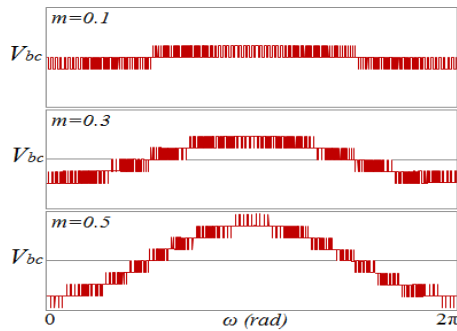
Fig. 15. Simulated line voltage of the inverter for low values of the modulation index
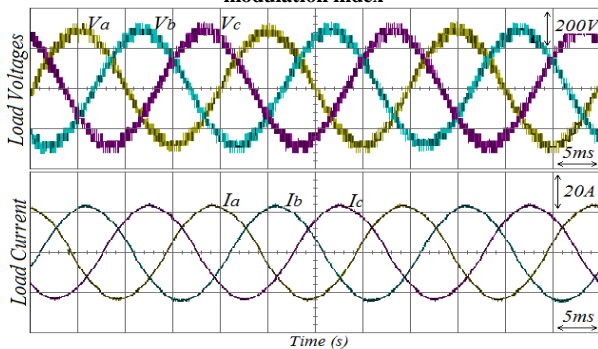
Fig. 16. Experimental load phases voltages and currents for m=1
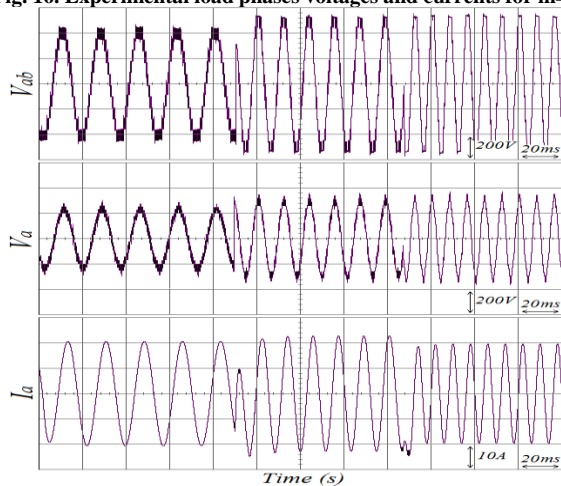
Fig.17. Experimental line voltages, phase voltages and currents of the load in three different conditions
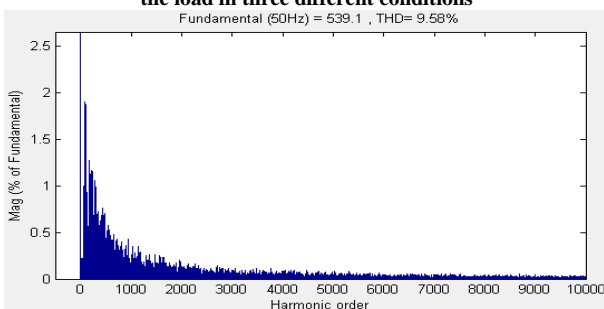
Fig. 18. Harmonic spectrum of the line voltage for $m=1$ and $f_o = 50$
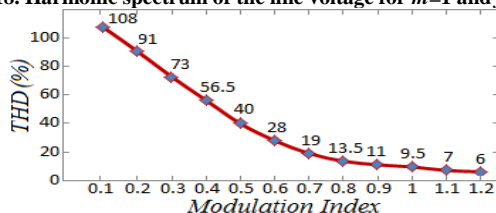
Fig. 19. THD values of the line voltages

Fig. 15 shows the simulated line voltage of the inverter for low values of the modulation index (m=0.1, m=0.3 and m=0.5). Fig. 16 shows the experimental load phases voltages and currents for m=1. Fig. 17 shows the experimental line voltages, phase voltages and currents of the load in three different conditions. Firstly, the reference signals V a1, fo and φ are 184 Volts, 62 Hertz and 0 degrees respectively and the inverter operates in linear modulation region. Then the inverter output transfers to the point Va1=237, fo=83 and φ=20° operating in overmodulation region. Finally, the inverter operation passes to staircase mode (Va1=250, fo=122 and φ=55°). This figure shows easy and continuously extension of the CHBI operation to overmodulation region with the proposed method. Fig. 18 shows the harmonic spectrum of the line voltage for m=1 and fo = 50. The THD curve of the line voltages in terms of the modulation index is shown in Fig. 19. The simulation and experimental results demonstrate valid performance of the proposed modulation method.

5. CONCLUSIONS

A novel modulation method for voltage control of CHBIs was proposed. The main contributions of this paper are summarized as follows:

1) The selection of the switching vectors to synthesize the reference vectors is simple. The proposed method has lower computational overhead and memory requirements compared with SVPWM-based methods.

2) The proposed method conveniently selects the switching vectors in the overmodulation condition and hence results in a smooth transition from linear modulation to overmodulation region without requiring lookup tables.

3) The switching algorithm is similar to hybrid multilevel inverters and achieves improved efficiency for the inverter.

The proposed method has been applied to a simulated and laboratory-built CHBI. The simulation and experimental results were carried out in different conditions and the results verify the effectiveness of the proposed algorithm.

REFERENCES

[1] B. Wu, "HIGH-POWER CONVERTERS AND AC DRIVES" New Jersey: John Wiley & Sons; 2006.

[2] M. Nikpayam et al., "Vector control methods for star-connected three-phase induction motor drives under the open-phase failure", *J. Oper. Autom. Power Eng.*, vol. 10, no. 2 pp. 155-164, 2022.

[3] F. Mohammadi et al., "Design of A single-phase transformerless grid connected PV inverter considering

reduced leakage current and LVRT grid codes", *J. Oper. Autom. Power Eng.*, vol. 9, no. 1, pp. 49-59, 2021.

[4] Q. M. Attique, Y. Li and K. Wang, "A survey on space-vector pulse width modulation for multilevel inverters", *CPSS Tran. Power Electron. App.*, vol. 2, no. 3, pp. 226-236, 2017.

[5] X. Wu et al., "A simplified space vector pulsewidth modulation scheme for three-phase cascaded h-bridge inverters", *IEEE Trans. Power Electron.*, vol. 35, no. 4, pp. 4192-4204, 2020.

[6] R. Rabinovici et al., "Series space vector modulation for multi-level cascaded H-bridge inverters," *IET Power Electron.*, vol. 3, no. 6, pp. 843–857, 2010.

[7] A. Mohamed, A. Gopinath and M. R. Baiju, "A Simple space vector PWM generation scheme for any general n-level inverter", *IEEE Trans. Ind. Electron.*, vol. 56, no. 5, pp. 1649-1656, 2009.

[8] I. Ahmed et al., "Simplified space vector modulation techniques for multilevel inverters", *IEEE Trans. Power Electron.*, vol. 31, no. 12, pp. 8483-8499, 2016.

[9] A. Ovalle, M. Hernández and G. Ramos, "A flexible nonorthogonal reference frame based SVPWM framework for multilevel inverters", *IEEE Trans. Power Electron.*, vol. 32, no. 6, pp. 4925-4938, 2017.

[10] P. Chamarthi, P. Chhetri and V. Agarwal, "Simplified implementation scheme for space vector pulse width modulation of n-level inverter with online computation of optimal switching pulse durations", *IEEE Trans. Ind. Electron.*, vol. 63, no. 11, pp. 6695-6704, 2016.

[11] I. Ahmed and V. B. Borghate, "simplified space vector modulation technique for seven-level cascaded H-bridge inverter", *IET Power Electron.*, vol. 7, no. 3, pp. 604-13, 2014.

[12] H. Zhang et al., "Fast and simple space vector modulation method for multilevel converters", *IET Power Electron*, vol. 13 no. 1, pp. 14-22, 2020.

[13] J. Hu, J. Lin and H. Chen, "A discontinuous space vector PWM algorithm in ABC reference frame for multilevel three-phase cascaded h-bridge voltage source inverters", *IEEE Trans. Ind. Electron.*, vo. 64, no. 11, 2017.

[14] X. Yuan, Y. Gao and Y. Li, "A fast multilevel SVPWM method based on the imaginary coordinate with direct control of redundant vectors or zero sequence components", *IEEE Open J. Ind. Electron. Soc.*, vol. 1, pp. 355-366, 2020.

[15] H. Lin et al., "A fast and flexible nearest-level-equivalent space vector modulation algorithm for three-phase multilevel converters", *Elec. Power Energy Sys.*, vol. 118, pp.1-10, 2020.

[16] M. A. Menon and B. Jacob, "A simplified space vector pulse density modulation scheme without coordinate transformation and sector identification", *IEEE Trans. Ind. Electron.*, vol. 69, no. 5, pp. 4431-4439, 2022.

[17] X. Guo, M. He and Y. Yang, "Over modulation strategy of power converters: a review", *IEEE Access*, vol. 6, pp. 69528-69544, 2018.

[18] A. K. Gupta and A. M. Khambadkone, "A general space vector pwm algorithm for multilevel inverters, including operation in overmodulation range", *IEEE Trans. Power Electron.*, vol. 22, no. 2, pp. 517-526, 2007.

[19] S. Pramanick et al., "Extending the linear modulation range to the full base speed using a single DC-Link multilevel inverter with capacitor-fed h-bridges for IM drives", *IEEE Trans. Power Electron.*, vol. 32, no. 7, pp. 5450-5458, 2017.

[20] M. D. Manjrekar, P. K. Steimer and T. A. Lipo, "Hybrid multilevel power conversion system: a competitive solution for high-power applications", *IEEE Trans. Ind. App.*, vol. 36, no. 3, pp. 834-841, 2000.

[21] M. Perez et al., "Power distribution in hybrid multi-cell converter with nearest level modulation", *IEEE Int. Symp. Ind. Electron.*, 2007.

[22] T. Qanbari and B. Tousi, "Single-source three-phase multilevel inverter assembled by three-phase two-level inverter and two single-phase cascaded h-bridge inverters", *IEEE Trans. Power Electron.*, vol. 36, no. 5, pp. 5204-5212, 2021.

[23] B. Kumar and M. Lokhande, "Analysis of PWM techniques on multilevel cascaded H-Bridge three phase inverter", *Recent Develop. Control Autom. Power Eng.*, 2017.